Combined scanning tunneling microscopy and reflectance anisotropy spectroscopy study of self-organized anisotropic cobalt nanodots on a vicinal Au(111) surface

N. Witkowski* and Y. Borensztein†
Laboratoire d'Optique des Solides, UMR-CNRS 7601, Université Pierre et Marie Curie, 4 Place Jussieu, 75252 Paris Cedex 05, France

G. Baudot, V. Repain, Y. Girard, and S. Rousset‡
Groupe de Physique des Solides, UMR-CNRS 7588, Universités Paris 6 et Paris 7, 2 Place Jussieu, 75251 Paris Cedex 05, France
(Received 9 April 2004; published 23 August 2004)

We report on a combined study of two dimensional long-range ordered growth of anisotropic cobalt nanostructures on Au(11,12,12) by means of *in-situ* scanning tunneling microscopy (STM) and reflectance anisotropy spectroscopy (RAS). The main structure observed in the RA spectra originates from the plasma resonances that occur in the anisotropic Co nanostructures. A simple model allows us to reproduce the general behavior of this structure, in agreement with the Co nanostructure morphologies extracted from the STM images. Moreover, a real-time investigation by RAS during Co deposition at a fixed photon energy allows us to follow the self-organized growth regimes. RAS appears to be a versatile technique which is sensitive to the anisotropic shape of metal nanodots.

DOI: 10.1103/PhysRevB.70.085408 PACS number(s): 68.65.−k, 81.16.−c, 78.68.+m, 78.67.Bf

I. INTRODUCTION

Many efforts have been devoted to miniaturization in microelectronic and storage media devices in the last decade. Up to now the production of nanostructures was achieved in a top-down approach using lithographic methods. But within these techniques, the device fabrication for electronics at sub-100 nm dimension becomes a real challenge.[1] A new promising way to produce nanoscale structures is to use a bottom-up approach where self-organization[2] and ordered growth phenomena[3] are used. This approach allows to organize regular nanostructures over macroscopic areas with a high spatial density. Recently, the growth of self-organized nanostructures of cobalt has been achieved on vicinal Au(111) surfaces with a high degree of long range order.[4,5] This has been extensively demonstrated on the Au(788) substrate which is a stable Au(111) vicinal surface, spontaneously patterned in two dimensions at a nanometer scale. This is due to a surface reconstruction crossing a periodic steps array. The coherence length of this pattern is kept all over the macroscopic sample. This pattern is used as a template for the growth of long-range ordered nanodots array over a wide temperature range.[6] At room temperature, the islands shape is highly anisotropic. The cobalt nanostructures are flat parallelepipeds [2 monolayers (ML) thick], elongated along the steps. Their sizes and anisotropic shapes depend on the coverage. Since they are organized on a periodical rectangular array, they are all oriented in the same way all over the macroscopic size of the sample surface. Therefore, they provide a unique model system in order to study physical properties of nanostructures which depend on the size and shape.

We report here the first application of reflectance anisotropy spectroscopy (RAS) to regular self-organized nanostructures. RAS measures the difference of the complex optical reflectance for polarization along two perpendicular axes. It has been extensively used in the field of semiconductor surface analysis[7,8] including reconstruction and phase transition, and also in semiconductor crystal growth.[9] This surface sensitive technique is now also commonly used to investigate anisotropic (110) metal surfaces[10] and more recently vicinal (111) surfaces.[11] It has been also used to study the growth of thick films formed by disordered metal islands on a semiconductor substrate.[12] Moreover surface differential reflectivity spectrocopy (SDRS), another surface sensitive optical spectroscopy, has been shown to be very sensitive to the morphology of metallic nanoparticles on different kinds of surfaces.[13,14] Indeed, it is well known that in small particles of free-electron metals like silver, the surface plasmons can be excited by ultraviolet or visible polarized light.[13,15] The corresponding optical spectra present plasma resonances whose intensities, shapes, and positions strongly depend on the morphology of the particle assembly. In Co particles, the surface plasmon resonances are strongly damped due to the *d* character of the conduction band but still exist.

We have performed a combined study of self-organized cobalt nanostructures onto vicinal Au(11,12,12) surface by means of *in-situ* scanning tunneling microscopy (STM) and RAS. The Au(11,12,12) surface displays the same nanopattern as the Au(788) surface, due to the systematic crossing between steps and reconstruction. Therefore, when Co is deposited onto Au(11,12,12), the particles have all about the same morphology and are regularly organized leading to an average anisotropic surface. A simple dipolar model, which uses the morphological data extracted from STM images, allows us to satisfactorily reproduce the experimental RA spectra. Moreover, by use of a real-time investigation of RAS during the cobalt deposition at a fixed photon energy, corresponding to the Co plasmonlike resonance, we can monitor the different growth regimes of the cobalt nanostructures.

II. EXPERIMENTAL DETAILS

The experiments were carried out in an ultrahigh vacuum system operated at low 10^{-11} Torr which is composed of a preparation chamber equipped with facilities for low electron energy diffraction (LEED), Auger electron spectroscopy, ion sputtering, thermal evaporation, and an analysis chamber where STM at variable temperature can be performed. The vicinal substrate is a Au(11,12,12) single crystal disorientated by 2.3° with respect to the (111) surface, and has been prepared following the same procedure as described in Ref. 5. After several cycles of argon sputtering followed by subsequent annealing at 800 K, a sharp LEED pattern was observed and no contamination was visible in Auger spectroscopy. The procedure to evaporate cobalt and calibrate the deposition rate is the same as described in Ref. 5. Co deposition, RAS measurements and STM images were taken *in-situ* at room temperature. The RAS spectra were recorded through a low-strain quartz window by use of a home-made apparatus, similar to the spectrometer developed by Aspnes.[16] We have measured here the anisotropy of the surface reflectance given by the formula

$$\frac{\Delta r}{r} = 2\frac{r_{[\bar{2}11]} - r_{[01\bar{1}]}}{r_{[\bar{2}11]} + r_{[01\bar{1}]}}, \tag{1}$$

where $r_{[\bar{2}11]}$ and $r_{[01\bar{1}]}$ are the complex reflectances along the directions $[\bar{2}11]$ and $[01\bar{1}]$, respectively, as indicated on Fig. 1.

III. RESULTS AND DISCUSSION

In this section we present RAS results of various Co coverage deposited on Au(11,12,12). RA spectra were recorded right after the Co deposition and the sample was then transfered to the STM chamber for topographic acquisition. After imaging, the sample was brought back to the preparation chamber for additional Co deposition. This allows us to interpret the RAS results in terms of morphological modifications characterized by a quantitative statistical analysis of STM images.

The Au(11,12,12) surface is composed of 5.9 nm wide terraces separated by monoatomic steps. Each terrace displays alternative fcc and hcp packed domains separated by discommensuration lines running across the steps as it has been shown for the same kind of substrates.[4,5] The reconstructed surface can therefore act as a regular template and lead to an organized growth of cobalt nanodots with a good long-range order.[4] The lattice parameters of the dot array are 5.9 nm in the $[\bar{2}11]$ direction, which corresponds to the terrace width and 7.2 nm in the $[01\bar{1}]$ direction, which corresponds to the reconstruction period. Despite the very different sizes of RAS and STM probes, we want to point out that the macroscopic coherence length of the Co nanodots array allows to extract morphological informations (density, size, aspect ratio, etc.) from the STM images reliable for the analysis of RAS measurements. The top spectrum of Fig. 1(e) is the optical anisotropy signal measured on the clean Au(11,12,12) surface. The weak anisotropy observed with

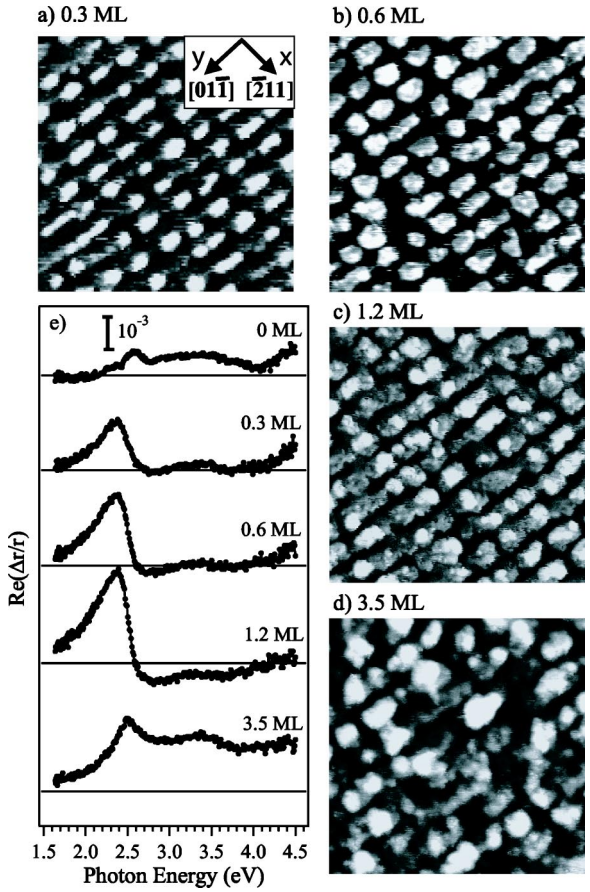

FIG. 1. RA spectra for various coverages of Co (e) and corresponding STM images (50 nm × 50 nm) recorded at the same coverage rate [(a), (b), (c), (d)].

the small feature around 2.6 eV corresponds to the edge of the interband transition in gold and likely originates from steps at the surface. Indeed, the optical response of stepped surfaces is different when the electromagnetic field is along or perpendicular to them as it has been recently demonstrated on Cu stepped surfaces.[11] This optical signal is also similar to what has been already observed for Au(110)[17–20] surfaces and other noble metals.[10,21]

Figure 1(e) reports RA spectra and the corresponding STM images for different Co mass coverages [0.3 ML (a), 0.6 ML (b), 1.2 ML (c), and 3.5 ML (d)], measured in equivalent monolayers where the thickness of 1 ML is 0.203 nm. The first striking observation is that the spectra corresponding to 0.3 ML, 0.6 ML, and 1.2 ML of cobalt are quite similar and display an increasing positive structure at 2.35 eV. For higher photon energies, the spectra are almost structureless and only a small anisotropy is observed. For coverages of 0.3 ML and 0.6 ML, STM images show that flat cobalt islands of 2 ML thickness (0.407 nm) are regularly organized onto the terraces parallel to the discommensurate lines, as it has been already reported in a previous study on a similar vicinal surface.[4,5] The Co clusters display asymmetric shapes elongated along the step directions. Their average size is estimated at 3.2 nm × 3.8 nm for 0.3 ML and 4.5 nm × 5.3 nm for 0.6 ML. When increasing cobalt coverage, the islands grow both along the steps and across the

terraces. The coalescence mainly occurs along the steps, leading to discontinuous lines parallel to the steps, as it can be observed for 1.2 ML coverage [Fig. 1(c)]. We thus deduce that the large feature at 2.35 eV, which develops with Co deposition, is characteristic of the Co nanocluster morphology as it will be demonstrated below. The spectrum obtained for larger cobalt coverage (3.5 ML) displays different features. This RA spectrum looks like the spectrum recorded on the clean gold surface with a larger intensity. The STM image recorded for 3.5 ML of Co shows that the islands coalesce in both directions leading to a continuous Co film with a rough surface. From the optical point of view, due to this 2D coalescence the nanoparticle character disappears. The presence of a continuous cobalt layer on the surface yields apparently some enhancement of the intrinsic optical anisotropy of the gold vicinal surface originating from the steps. Although the origin of this effect is not yet understood, it demonstrates the ability of RAS to probe the anisotropy of buried interfaces, which is difficult to achieve with other techniques.

In order to correlate the morphology of the Co nanostructures with the pronounced feature around 2.35 eV observed in RAS, we use a quasistatic model to calculate the optical response of the gold surface covered with Co particles. The optical response of Co particles, considered as ellipsoids, to an applied electromagnetic field, is described in the dipolar approximation.[22] As it will be shown below, the optical signal, observed when increasing the Co deposition, originates from the plasmonlike electronic resonances that occur in the flat anisotropic particles. These resonances are damped compared to free-electron metals, but are still present in the cobalt nanoclusters. In the model we use, the interaction between the cobalt clusters and the gold surface is neglected, since it has been demonstrated theoretically that this interaction with the substrate vanishes for the limiting case of a very flat particle, so that the polarizability becomes equal to a free particle polarizability.[23] Consequently, the RA spectra recorded for Co deposited on gold surfaces can be considered as the sum of the RAS signal coming from the clean gold surface and the RAS signal of the self-sustained array of cobalt nanoclusters. The RA spectra contribution due to cobalt particles is then obtained by substracting the clean gold spectrum; results are presented in Fig. 2(a) for two different coverages: 0.3 ML and 0.6 ML, respectively. Both spectra are clearly dominated by a large positive structure around 2.35 eV which increases with Co coverage. To understand the origine of this feature, let us consider the polarizability tensor of an isolated ellipsoidal particle within the quasistatic approximation, valid for particle sizes much smaller than the wavelength of light, which is the case here for the Co particles. This polarizability tensor depends on the particle shape and can be written as follows:

$$\alpha_{ii} = \frac{V}{4\pi} \frac{\epsilon(\omega) - 1}{1 + (\epsilon(\omega) - 1)L_i}, \tag{2}$$

where V is the volume of the particle, $\epsilon(\omega)$ is the complex dielectric function of the metal particle [here, Co (Ref. 24)] and L_i is the depolarization factor along the i direction ($i = x, y, z$ and $0 < L_i < 1$), which can be calculated easily for an ellipsoid.[22] When considering a metal whose dielectric function has a small imaginary part with respect to the real part, the polarizability displays a sharp resonance when the denominator is close to zero, i.e., for $\epsilon(\omega) \simeq 1 - (1/L_i) < 0$. This corresponds to a surface-plasmon resonance in the particle along the i direction.[15] In the case of Co, where $\mathrm{Im}[\epsilon(\omega)]$ has large values, the surface plasmon resonance can exist too but it is strongly damped.

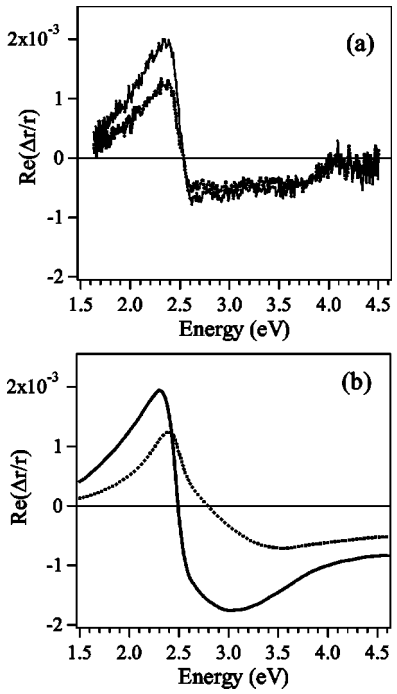

FIG. 2. (a) RA spectra of Co nanostructure contribution for 0.3 ML (dotted line) and 0.6 ML (solid line); (b) calculated spectra for corresponding coverage.

We present in Fig. 3 the imaginary parts of the polarizability tensor calculated for a Co ellipsoid, whose shape corresponds to the mean shape of the actual particles obtained for the coverage of 0.6 ML (i.e., with axes $a_x \approx 4.5$ nm, $a_y \approx 5.3$ nm, and $a_z = 0.407$ nm, respectively). They are compared to the polarizability calculated for a Co sphere. In this latter case, no plasma resonance is obtained in the near UV-

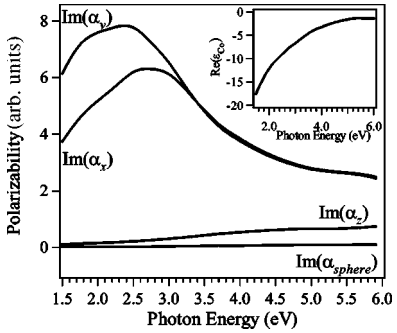

FIG. 3. Imaginary part of the polarizability tensor calculated for a cobalt ellipsoid, with axes equal to $a_x = 4.5$ nm, $a_y = 5.3$ nm, and $a_z = 0.407$ nm, and for a cobalt sphere. The real part of the dielectric function of cobalt is shown in the inset. (See Ref. 28.)

visible range under investigation (1.5–6 eV). On the contrary, for the flat particles, the polarizabilities along the largest dimensions of the particles (i.e., x and y) display indeed broad surface plasmon resonances, about 2 eV wide, located around 2.8 eV and 2.4 eV, respectively. It is worthwhile to note that the excitation of surface plasmons along x and y directions in these Co particles is due to their particularly flat shape. Indeed, the depolarization factors along x and y are $L_x=0.066$ and $L_y=0.052$, respectively, which permits the resonance to occur between 2 and 3 eV, where $\mathrm{Re}[\epsilon(\omega)]$ has large negative values, as seen in the inset of Fig. 3.[28] In the sphere case, the value of L is $1/3$ and no resonance is obtained. For the same reason, no resonance is visible in the z direction, for which the depolarization factor is $L_z=0.882$. Moreover, the resonance along the shorter dimension x is located at higher energy than the one along the longer dimension y, which is due to the slightly larger depolarization factor along x than along y. This difference between L_x and L_y is clearly the origin of the anisotropy measured on our system of particles.

From the polarizability of the particles, and considering that all particles are identical and distributed in a rectangular array of parameters 5.9 nm and 7.2 nm, the optical reflectance anisotropy of the assembly of Co particles on the Au substrate is calculated, by use of the following formula:

$$\frac{\Delta r}{r}=\frac{r_x-r_y}{r}=-8i\pi\frac{\omega}{c}N\frac{\alpha_{xx}^{\star}-\alpha_{yy}^{\star}}{\epsilon_{\mathrm{Au}}-1} \tag{3}$$

where N is the nanoparticle surface density, ϵ_{Au} is the bulk dielectric function of the gold substrate,[25] and $\alpha_{xx}^{\star}$ and $\alpha_{yy}^{\star}$ are the effective polarizabilities of the nanoparticles including the electromagnetic interaction between the particles within the dipolar approximation.[26,27]

At this point, it is necessary to discuss the relationship between the shape of the particles, the amount of cobalt and the corresponding RA spectra. The spectra mainly depend on two parameters describing the morphology of the particles: (i) their flatteness, (ii) their slightly elongated shape. The effect of the different parameters is analyzed below for a coverage of 0.6 ML with a particle density determined from STM image and, thus, an average defined volume for each particle. Figures 4(a)–4(c) give RA spectra calculated for particles with heights equal to 0.407 nm (2 ML), 0.610 nm (3 ML), and 0.814 nm (4 ML), respectively, and with different aspect ratios a_x/a_y (AR) indicated in the caption. The first piece of information obtained from this figure is that, for a given height, the intensity of the signal increases rapidly when the ratio a_x/a_y decreases. This was expected, as RAS is a measure of the anisotropy of the particles: the more elongated the particles are, the larger the RA signal is. The comparison with the experiments [Fig. 2(a)] shows that the actual particles display a slight anisotropy but are not very much elongated. The second piece of information is that the shape of the spectra strongly depends on the height of the particles, given here in ML. This is due to the fact that, for a given couple of values (a_x,a_y), the corresponding depolarization factors L_x and L_y, therefore the locations of the plasmon resonances along x and y, are much affected by the third

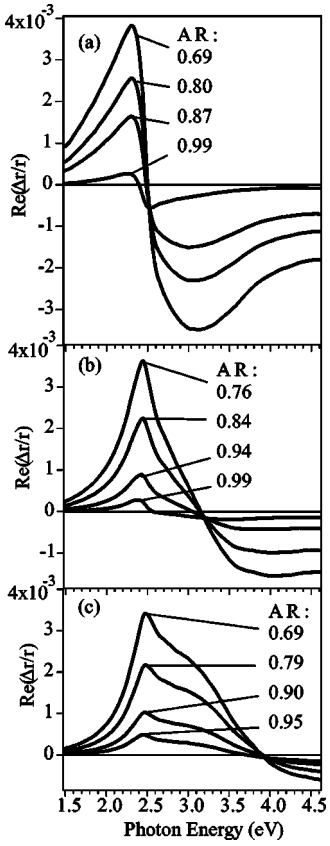

FIG. 4. RA spectra calculated for 0.6 ML coverage; the particles are distributed on a rectangular lattice of 5.9 nm×7.2 nm. (a) 2 ML thick particles, (b) 3 ML thick particles, (c) 4 ML thick particles. The aspect ratio (AR) is indicated for each spectrum.

dimension a_z of the particles. In conclusion, the analysis of Fig. 4 shows that a good agreement between the shapes of the experimental curves and the calculated ones, namely the strong peak at 2.3 eV and the fast decrease at 2.5 eV towards negative values, is obtained for the 2 ML thick island series, but not for the 3 ML and the 4 ML series. Moreover, we can determine rather precisely the average ratio a_x/a_y of the particles to be around 0.85, which is in excellent agreement with the observation by STM. Now, the effect of the total amount of Co has not been discussed in detail so far. From Eqs. (2) and (3), it can be seen that RAS is proportional to the total amount of Co (i.e., the volume V of the particles times the density of particles N), if the shape of the particles (therefore the L_i) is unchanged. This means that the Co coverage and the aspect ratio a_x/a_y are correlated parameters: RAS measurements alone do not permit us to determine completely the amount of Co and the exact shape of the particles. On the other hand, if the coverage is determined by another way, as it is the case here by use of a quartz microbalance, the comparison of the calculated curves obtained for different kinds of particles with the experimental data leads to a reasonable determination of the shape of the particles, i.e., of the relative dimensions of the ellipsoids. The additional knowledge, as obtained here from STM, either of the density of particles (therefore the volume of each particle) or of their height, yields the determination of the absolute dimensions of the particles.

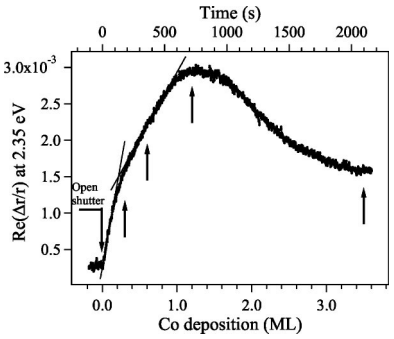

FIG. 5. Real time anisotropic signal at 2.35 eV during Co deposition. The corresponding RAS and STM images presented in Fig. 1 are indicated by arrows.

Figure 2(b) shows the RA spectra calculated for 0.3 ML and 0.6 ML coverages, where the dimensions of the 2 ML thick particles (a_x=3.18 nm and a_y=3.82 nm for the 0.3 ML, a_x=4.54 nm and a_y=5.35 nm for the 0.6 ML case) have been adjusted in order to get the best agreement with the experimental curves of Fig. 2(a), both in intensity and in shape. These dimensional parameters are identical to the average ones estimated from the analysis of the STM images presented in Figs. 1(a) and 1(b), respectively. The calculated curves reproduce rather correctly the main feature of the experimental data at 2.35 eV, that we can now clearly attribute to the anisotropy of the plasmon resonances in the cobalt clusters. The sign, the intensity and the energy of the experimental feature are reasonably well simulated. However some discrepancies occur in the calculated curves, especially for higher photon energies. Such differences could take their origines in the very simple model we used. Indeed, the clusters are described by ellipsoids whereas their shapes are likely less regular. Moreover no multipolar interaction between the particles has been taken into account nor the interaction between the particles and the substrate. Finally the polarizability tensor has been calculated using the bulk dielectric function of Co, whereas the dielectric function for small clusters could differ from the bulk one. In spite of these limitations, the rather good agreement between experiment and calculation proves that the main structure observed in the RA spectra originates from the anisotropic shape of the cobalt nanostructures. This shows that the RAS technique is a good tool to determine the asymmetric shape of self-organized nanoclusters, even in the case of *d* metals.

We have also used RAS to follow the formation of the Co nanostructures on the Au(11,12,12) surface, by recording the RA intensity during the cobalt deposition at the fixed photon energy of 2.35 eV, which corresponds to the maximum of the main structure. The real-time evolution of the anisotropic intensity versus time and Co coverage is plotted in Fig. 5. The arrows indicate the coverages for which both STM images and RA spectra have been recorded. Three different steps can be distinguished.

(1) A very fast linear increase of the anisotropy up to 0.2 ML right after the shutter opening.

(2) A slower increase between 0.2 ML and 1 ML.

(3) A saturation of the signal between 1 ML and 1.6 ML followed by a slow decrease approaching a limit value.

It can be noticed that the anisotropic intensity increases as soon as the shutter is opened, which indicates that the RAS technique is very sensitive to the initial formation of clusters in the subnanometer scale. The fast increase of the anisotropy up to 0.2 ML is not fully understood yet. It is tentatively attributed to the initial nucleation process, where the gold steps could be decorated by cobalt atoms. Above 0.2 ML, all the nuclei sites are occupied and the islands begin to grow with anisotropic shape, leading to the second growth stage in which the anisotropic signal increases slower. After 1 ML, the saturation of the signal is likely due to the beginning of the Co island coalescence across the steps. The RA spectra still display the structure associated to the plasmon resonance, indicating that the anisotropic character of the nanoclusters is preserved. For coverages larger than about 1.6 ML, the optical signal begins to decrease; this behavior characterizes the loss of the anisotropic character of the clusters. Indeed, because of the coalescence, the cobalt deposit becomes more isotropic, leading to a decrease of the surface plasmon resonance, and eventually to its disappearance. For large coverages of about 3.5 ML, the optical signal stabilizes and the corresponding RA spectrum is quite different from the previous ones [Fig. 1(e)], indicating that the cobalt film is no longer formed by individual anisotropic cobalt clusters.

In this study, RAS appears to be a suitable technique to investigate a model system of self-organized metallic nanoparticles on a surface. Even if the Co is a *d* metal where the plasmon resonances are damped, the RA signal allows us to evidence the presence of very flat metallic anisotropic particles slightly elongated along the steps with the same orientation. From the calculation, we did not evidence a strong lattice influence in the RA spectra due to particle interactions, which means that, in that particular system, the RAS is almost not sensitive to the self-organization of the particles. Another advantage of RA is the possibility to follow the *in-situ* growth of Co islands and the capability to identify the beginning of the coalescence, which is not an easy task with STM due to the convolution between the tip and the nanodots. Moreover, measurements of gold-covered Co nanoparticles, showing the same resonance due to Co islands (not shown here), makes the RAS a very convenient technique to characterize the anisotropic shape of buried particles, which is not possible with STM or other standard surface techniques.

IV. CONCLUSION

We have performed a combined study of the growth of self-organized Co nanostructures on Au(11,12,12) by means of *in-situ* scanning tunneling microscopy and reflectance anisotropy spectroscopy. We have demonstrated the complementarity of these two techniques in the understanding of anisotropic nanostructure growth. Namely, we have shown that the RA spectra obtained for different Co coverages can be explained by the presence of anisotropic Co nanoclusters regularly organized on the vicinal gold surface. An electrostatic model for describing the optical properties of the assembly of Co nanodots allowed us to attribute the main fea-

ture observed in the RA spectra to surface plasmon resonance in the particles, whose sign, intensity and position depend on the shape of the clusters. The so-determined dimensions of the particles are in excellent agreement with the ones extracted from the STM images. By using real-time RAS at a fixed photon energy during Co deposition, we have followed the growth process. After the initial nucleation, different regimes clearly appear: (i) the RA signal increase is attributed to the growth of cobalt nanostructure along the steps; (ii) after 1.2 ML the RA signal decreases since the coalescence of nanostructures occurs in two dimensions (i.e., across the steps). In the case of self-organized anisotropic nanostructures, RAS, which is a versatile technique, is proved to be very helpful to determine the shape of particles and to identify the stages of growth.

ACKNOWLEDGMENT

This work has been supported by the "Programme Matériaux" 2000–2002 of the CNRS.

*Electronic address: nadine.witkowski@los.jussieu.fr
†Electronic address: borens@ccr.jussieu.fr
‡Electronic address: rousset@gps.jussieu.fr

[1] W. Hinsberg, F. A. Houle, J. Hoffnagle, M. Sanchez, G. Wallraff, M. Morrison, and S. Frank, J. Vac. Sci. Technol. B **16**, 3689 (1998).
[2] V. A. Shchukin and D. Bimberg, Rev. Mod. Phys. **71**, 1125 (1999).
[3] H. Brune, M. Giovannini, K. Bromann, and K. Kern, Nature (London) **394**, 451 (1998).
[4] V. Repain, G. Baudot, H. Ellmer, and S. Rousset, Europhys. Lett. **58**, 730 (2002).
[5] V. Repain, G. Baudot, H. Ellmer, and S. Rousset, Mater. Sci. Eng., B **B96**, 178 (2002).
[6] S. Rohart, G. Baudot, V. Repain, Y. Girard, S. Rousset, H. Bulou, C. Goyhenex, and L. Proville Surf. Sci. **559**, 47 (2004).
[7] D. E. Aspnes and A. A. Studna, Phys. Rev. Lett. **54**, 1956 (1985).
[8] P. Chiaradia and G. Chiarotti, in *Photonic Probes of Surfaces*, edited by P. Halevi (Elsevier, Amsterdam, 1995).
[9] D. E. Aspnes, E. Colas, A. A. Studna, R. Bhat, M. A. Kozaand, and V. G. Keramidas, Phys. Rev. Lett. **61**, 2782 (1988).
[10] Y. Borensztein, W. L. Mochan, J. Tarriba, R. G. Barrera, and A. Tadjeddine, Phys. Rev. Lett. **71**, 2334 (1993).
[11] F. Baumberger, T. Herrmann, A. Kara, S. Stolbov, N. Esser, T. S. Rahman, J. Osterwalder, W. Richter, and T. Greber, Phys. Rev. Lett. **90**, 177402 (2003).
[12] N. Esser, A. M. Frisch, A. Röseler, S. Schintke, C. Goletti, and B. O. Fimland, Phys. Rev. B **67**, 125306 (2003).
[13] Y. Borensztein, R. Alameh, and M. Roy, Phys. Rev. B **50**, 1973 (1994).
[14] C. Beitia and Y. Borensztein, Surf. Sci. **402–404**, 445 (1998).
[15] U. Kreibig and M. Vollmer, *Optical Properties of Metal Clusters* (Springer-Verlag, Berlin, 1995).
[16] D. E. Aspnes, J. P. Harbison, A. A. Studna, and L. T. Florez, J. Vac. Sci. Technol. A **6**, 1327 (1988).
[17] V. Mazine, Y. Borensztein, L. Cagnon, and P. Allongue, Phys. Status Solidi A **175**, 311 (1999).
[18] B. Sheridan, D. S. Martin, J. R. Power, S. D. Barrett, C. I. Smith, C. A. Lucas, R. J. Nichols, and P. Weightman, Phys. Rev. Lett. **85**, 4618 (2000).
[19] K. Stahrenberg, T. Herrmann, N. Esser, W. Richter, S. V. Hoffmann, and P. Hofmann, Phys. Rev. B **65**, 035407 (2001).
[20] V. Mazine and Y. Borensztein, Phys. Rev. Lett. **88**, 147403 (2002).
[21] P. Hofmann, K. C. Rose, V. Fernandez, A. M. Bradshaw, and W. Richter, Phys. Rev. Lett. **75**, 2039 (1995).
[22] L. D. Landau and E. M. Lifshitz, *Electrodynamics of Continuous Media* (Pergamon, New York, 1960).
[23] P. A. Bobbert and J. Vlieger, Physica A **147**, 115 (1987).
[24] L. Ward, in *Handbook of Optical Constants of Solids II*, edited by E. D. Palik (Academic Press, San Diego, 1991).
[25] P. B. Johnson and R. W. Christy, Phys. Rev. B **6**, 4370 (1972).
[26] T. Yamaguchi, S. Yoshida, and A. Kinbara, Thin Solid Films **21**, 173 (1974).
[27] R. G. Barrera, M. del Castillo, G. Monsivais, P. Villaseñor, and W. L. Mochan, Phys. Rev. B **43**, 13 819 (1991).
[28] The resonance does not occur exactly for energy where the relation $\epsilon(\omega) \simeq 1-(1/L_{x,y})$ is fulfilled: the maximum of $\mathrm{Im}[\alpha]$, which corresponds to the actual plasmon resonance in the particle, is shifted because of the presence of the large imaginary part of the dielectric function $\epsilon(\omega)$.